

Damage threshold affected by the spatiotemporal evolution of femtosecond laser pulses in multilayer structures

Amir Khabazzi Oskouei,^a Matthias Lenzner,^{b,*} Luke A. Emmert,^a
Marco Jupé,^c Thomas Willemsen,^d Morten Steinecke,^c
Detlev Ristau^{b,c} and Wolfgang Rudolph^a

^aUniversity of New Mexico, Department of Physics and Astronomy,
Albuquerque, New Mexico, United States

^bLenzner Research LLC, Tucson, Arizona, United States

^cLaser Zentrum Hannover e.V., Hannover, Germany

^dLaseroptik Garbsen GmbH, Garbsen, Germany

Abstract. We propose a figure of merit that characterizes the femtosecond laser damage behavior of optical coatings. This figure of merit, based on the complete spatiotemporal evolution of the field in a multilayer system, can be included in optics design. The monochromatic intensity enhancement widely used in “electric field-engineering” is sufficient only in certain structures such as high-reflectivity quarter-wave mirrors. In more complex systems, for example, in group delay dispersion mirrors and frequency tripling mirrors, one should consider the actual (typically smaller) intensity enhancement produced by short pulses and the change (typically increase) of pulse duration within the stack. © 2022 Society of Photo-Optical Instrumentation Engineers (SPIE) [DOI: [10.1117/1.OE.61.7.071602](https://doi.org/10.1117/1.OE.61.7.071602)]

Keywords: laser-induced damage; femtosecond lasers; multilayers; multilayer design; optical coatings.

Paper 20211418SS received Dec. 2, 2021; accepted for publication Jan. 28, 2022; published online Apr. 23, 2022.

1 Introduction

The physical processes controlling laser-induced machining and material modifications are also responsible for undesired outcomes of laser–matter interactions, such as laser-induced damage (LID). A better understanding of the underlying mechanisms thus serves both the development of efficient and accurate laser processing technologies and optical components with higher laser-induced damage threshold (LIDT).

The push to ever-more-powerful pulsed laser systems producing sub-100-fs pulses continues to challenge limits of current optical elements such as dielectric coatings. A great deal of work has targeted the increase of their LIDT through improvements in materials and deposition modalities. These efforts include mixed oxide compositions,¹ nanolaminate structures,² and continuous interface deposition.³ Compared to damage by nanosecond pulses, LID by femtosecond pulses is more deterministic and reflects the intrinsic limits of the material.⁴ Damage models for single and multiple pulses have been able to explain main experimental findings. Chief among these are the scaling of the LIDT with bandgap and refractive index, respectively, as well as the pulse duration dependence.⁵ While many questions are still open, it is established that the LID initiating processes are controlled to the first order by the local laser intensity and pulse duration for 1-on-1 and S-on-1 illumination scenarios.⁶ These pulse parameters determine the process of energy deposition, a precursor to damage.⁷

In a multilayer optical coating, the value and location of the peak intensity are determined by the superposition of counterpropagating fields in the film stack. The ratio of the peak intensity

*Address all correspondence to Matthias Lenzner, matthias@lenzner.us

in the stack to the maximum incident pulse intensity is called the (field) intensity enhancement. For instance, in a quarter-wave stack of high and low index layers (i.e., a high-reflector), the peak intensity occurs at the interface of the first and second layers from the surface. Apfel suggested to improve the LIDT in a high reflector (HR) by modifying the top layer thicknesses to shift the peak intensity into a high bandgap (low index) layer.⁸ Another approach used top layers with higher intrinsic LIDT.^{1,9} Broadband mirror designs for subpicosecond pulses are now commonly optimized by minimizing the intensity enhancement in the low-bandgap layers.¹⁰⁻¹² Attempts have also been made to minimize specific detrimental nonlinear optical effects, for example, two-photon absorption.¹³

In all of these examples, the intensity enhancement was typically calculated for monochromatic input at the center wavelength of the pulse spectrum. This is justified if the pulse duration does not change in the regions of high field intensity enhancement, which is the case for optics that show low group delay dispersion (GDD). Examples include high-reflectors derived from quarter-wave stacks. For more complex structures, such as group delay dispersion mirrors (GDDMs) and frequency tripling mirrors (FTMs),¹⁴ this condition is no longer true.

In this paper, we discuss how the pulse duration and the pulse intensity enhancement behave within the film stack and how this can affect the LIDT. We will explore the limits of optimizing for intensity enhancement using the monochromatic approximation, and we will suggest an approach to include the LIDT behavior for short pulses into a multilayer design merit function.

2 Figure of Merit Characterizing Damage Thresholds of Stacks of Films

To define an LID merit function of a multilayer coating, let us consider thin films stacked in the positive z direction starting from air. The intensity $I(z) = \langle E(t, z)^2 \rangle$ has typically been used as a measure of the local laser exposure within the coating stack. The prefactor containing the dielectric constant is omitted to avoid discontinuities at the interfaces. Here, E is the real electric field and $\langle \rangle$ means time average over an optical period, which leads to a time constant quantity if monochromatic (CW) input is used. The implicit assumption so far has been that LIDT or other detrimental material modifications can ultimately be traced to the intensity.

If we assume that the damage behavior of the film materials is known and can be characterized by a tangible physical quantity reaching a critical value at the LIDT, the ratio between this quantity and its critical value can be introduced as an LIDT predictor when designing the mirror. Current femtosecond LID models and experimental data suggest that this quantity can be the energy density per area (fluence F). We will therefore simply use the ratio of local fluence $F(z)$ and the critical fluence (LIDT) F_c to construct the figure of merit M :

$$M = \max \left\{ \frac{F(z)}{F_c(z)} \right\}. \quad (1)$$

Note that the threshold fluence F_c varies with z because of the varying materials within a multilayer system and because the LIDT F_c is also a function of the local pulse duration $\tau_p(z)$. Damage will be initiated at a certain depth in the stack z_m where the ratio F/F_c is maximum for given incident pulse parameters. At this location, F reaches the critical value F_c first when the incident fluence is increased.

Local fluence and pulse duration are determined by the parameters of the incident pulse and the film sequence. Each spectral component of the incident pulse forms a counterpropagating wave. The superposition of these spectral components determines the local intensity, which can be expressed mathematically as

$$I(z, t) = \hat{I}_0 |\text{IFT}\{\tilde{E}(z, \omega)\}|^2, \quad (2)$$

where IFT denotes inverse Fourier transform and \hat{I}_0 is the incident peak intensity. $\tilde{E}(z, \omega)$ is the (normalized) field amplitude at frequency ω and position z , which can be calculated from standard matrix optics from the known spectral field of the incident pulse and the properties (refractive indices and thicknesses) of the film sequence.¹⁵

The ratio of local intensity and incident peak intensity

$$Q(z, t) = \frac{I(z, t)}{\hat{I}_0} = |\text{IFT}\{\tilde{E}(z, \omega)\}|^2, \quad (3)$$

is the intensity enhancement. At position z in the film stack, the intensity enhancement is maximum at a certain time t_z . The global maximum intensity enhancement $\hat{Q} = \max\{Q(z, t)\} = Q(z_m, t_m)$ occurs at location z_m and time t_m . In terms of the intensity enhancement, the local fluence can be expressed as

$$F(z) = \hat{I}_0 \int Q(z, t) dt. \quad (4)$$

For further analysis of the merit function, Eq. (1), we need to specify $F_c(z)$ governing the LIDT behavior of the coating material. This function can be obtained from LIDT measurements on single films. For standard metal oxides, as they are routinely used in dielectric coatings from the near UV to near IR, measurements suggest an LIDT scaling law $F_c \approx [a + bE_g(z)]\tau_p^\kappa(z)$,⁵ where $\kappa \approx 0.3$. The parameters a and b weakly depend on the deposition conditions. The z dependence enters through the bandgap E_g of the film materials, which is different for the high and low index layers, and the local pulse duration. This phenomenological law also applies to composite (binary) oxides with tunable bandgap.¹⁶ With this F_c , the merit function can be written as

$$M(z_m) = \max \left\{ \frac{F(z)}{[a + bE_g(z)]\tau_p^\kappa(z)} \right\}. \quad (5)$$

An estimate for the local pulse duration $\tau_p(z)$ can be obtained from the ratio of fluence and peak intensity $F(z)/I(z, t_z)$, which in terms of the intensity enhancement can be expressed as

$$\tau_p(z) = \frac{\int Q(z, t) dt}{Q(z, t_z)}. \quad (6)$$

Here, we made use of Eqs. (3) and (4). Using this pulse duration and Eq. (4) for the fluence, the merit function Eq. (5) becomes

$$M(z_m) = \hat{I}_0 \max \left\{ \frac{Q(z, t_z)^\kappa [\int Q(z, t) dt]^{1-\kappa}}{a + bE_g(z)} \right\}. \quad (7)$$

Since \hat{I}_0 is constant, we have a merit function that solely depends on parameters of the incident pulse and film stack lumped into the intensity enhancement Q and the bandgap E_g of the materials used. It is obvious that increasing the input peak intensity \hat{I}_0 to a critical value will eventually lead to $M = 1$ (damage) at a certain position z_m .

The common monochromatic approach in mirror design is sufficient when the pulse duration does not change within the stack $\tau_p(z) = \tau_p(0)$ and $\hat{Q}_{\text{mon}} \approx \hat{Q}$. As will be discussed below, this is valid for relatively simple structures such as quarter-wave mirrors (QWM's) but not true for more complex mirrors such as GDDMs and FTMs.

3 Comparison of Different Mirror Architectures

Figure 1 shows the intensity enhancement $Q(z, t_m) = I(z, t_m)/\hat{I}_0$ (left) and the pulse duration in the stack (right) for a 40-fs (Gaussian) input pulse for four different mirrors: two HRs, a GDDM, and an FTM. The mirror properties are summarized in Table 1. Note, the maximum enhancement value for each mirror corresponds to \hat{Q} .

The design of mirror (b) was obtained from a computer search starting from a quarterwave stack. The merit function minimized during the optimization was the monochromatic intensity

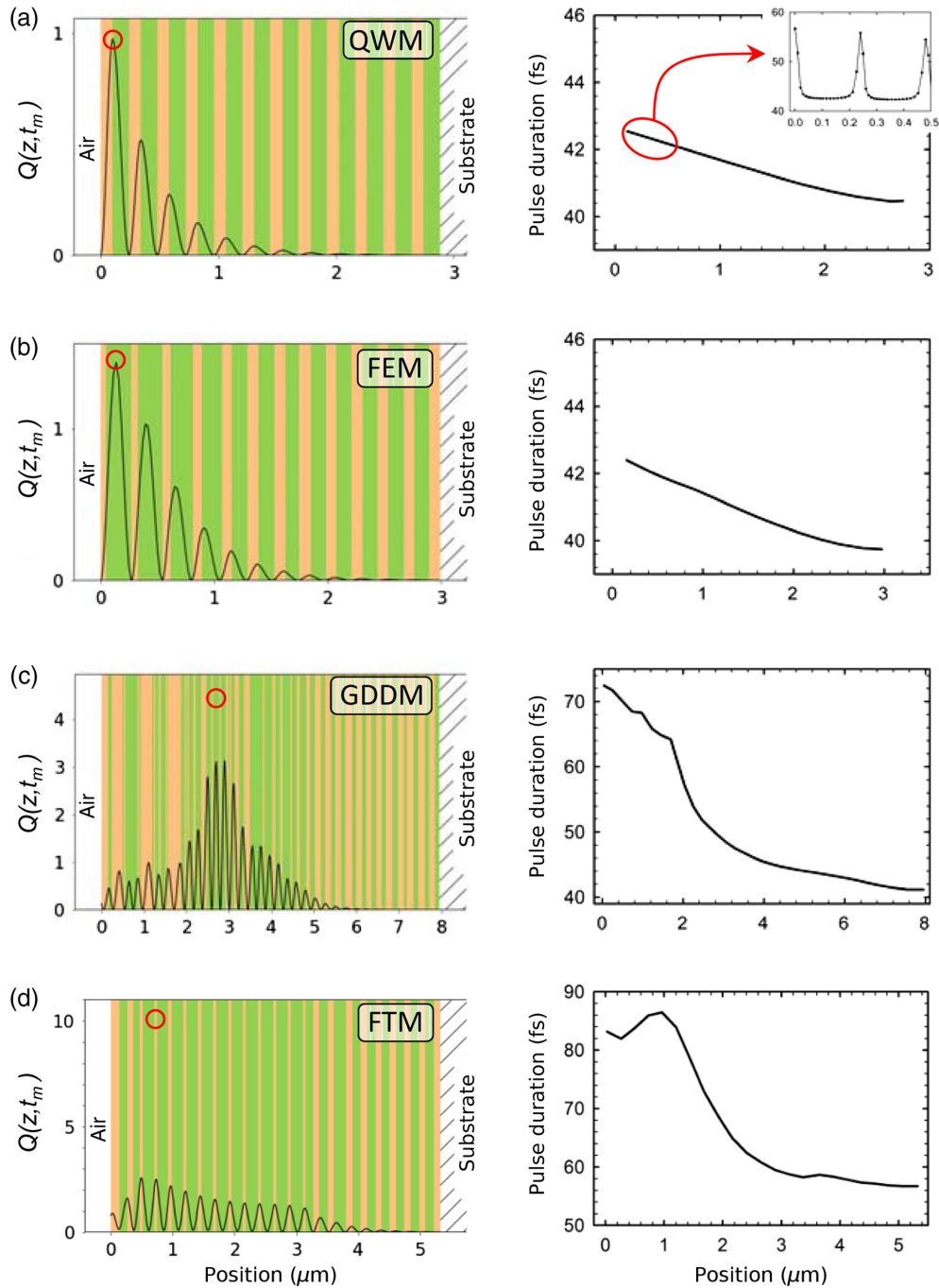


Fig. 1 Left: Intensity enhancement $Q(z, t_m)$ inside the mirror at time t_m produced by a 40-fs incident Gaussian pulse. The red circles show the intensity enhancement Q_{mon} , calculated for monochromatic input at the center wavelength, (a), (c) 820 nm and (b) and (d) 815 nm. Right: Pulse duration $\tau_p(z)$ in the stack according to Eq. (6). (a) QWM, (b) field-engineered high-reflecting mirror (FEM), (c) GDDM, and (d) FTM. The mirror properties are summarized in Table 1, the sequence of layers can be deduced from there. Except for the inset, the pulse durations in the vicinity of the field nodes are omitted (see text for a detailed explanation). Note that for a Gaussian pulse with a duration of 40 fs (FWHM), $\tau_p = 42.6$ fs.

enhancement \hat{Q}_{mon} in the high-index layer under the condition that the reflectance $R > 0.995$ over a predefined bandwidth $\Delta\lambda = 80$ nm. The result was a refined solution of the intuitive approach used in Ref. 8. Information about the details of the GDDM can be found in Ref. 17. The FTM was designed using an algorithm described in Ref. 18.

Table 1 Properties of the mirrors (a) to (d) used in Fig. 1.

Mirror	Architecture S: fused silica substrate	Bandwidth $R > 99.5\%$
(a) QWM quarterwave HR	$[\text{Ta}_2\text{O}_5, \text{SiO}_2]^{12}$ S	764 to 883 nm
(b) FEM field-engineered HR	$[\text{Ta}_2\text{O}_5, \text{SiO}_2]^{12}$ $[\text{Ta}_2\text{O}_5]$ S	772 to 858 nm
(c) GDDM (-200 fs^2)	$[\text{Ta}_2\text{O}_5, \text{SiO}_2]^{37}$ S	759 to 914 nm
(d) FTM	$[\text{HfO}_2, \text{SiO}_2]^{22}$ $[\text{HfO}_2]$ S	n. a.

Mirrors (a) and (b) show very little difference between the intensity enhancement of pulsed and CW input. The pulse duration was essentially constant throughout the stack, in particular in the high-intensity regions. The slight decrease in pulse duration as defined in Eq. (6) with increasing z is accompanied by a flattening of the pulse spectrum. The latter is a result of a smaller penetration depth into the stack of spectral components near the central wavelength that defines the thickness of the quarterwave layer. The field-engineered solution (FEM) found by the computer search showed a decrease in M by about a factor of 2 due to shifting \hat{Q} into the low-index material, suggesting a corresponding increase of the LIDT for femtosecond pulses.

The periodic increase of the pulse duration shown in the inset of Fig. 1(a) occurs near the nodes of the standing wave. At the nodes, the field spectrum shows a dip at the center frequency leading to a broader intensity distribution in the time domain (greater τ_p). Similar increases of τ_p occur in all mirrors. Since the overall intensities are low near the field nodes, these regions are not locations of LID initiation and have therefore been omitted in the graphs for clarity.

The situation is more complex in the GDDM and FTM where the pulse duration changes considerably within the stack. For these two mirrors, Fig. 2 shows the maximum intensity enhancement \hat{Q} as a function of the input pulse duration, for the low and high index layers. As expected, for long pulses, the monochromatic limit is reached, $\hat{Q} \rightarrow \hat{Q}_{\text{mon}}$.

The fact that \hat{Q} for pulses is smaller than the monochromatic limit is a result of dispersion. The different components of the pulse spectrum do not necessarily add up in phase at any position in the film stack if one starts with a bandwidth-limited pulse. Examples of the full spatiotemporal evolution of $E(z, t)$ in various mirrors and for different pulse durations can be viewed in Ref. 19.

Figure 3 summarizes relevant results for a dispersive mirror as commonly used, for example, in femtosecond amplifiers and compressors. This mirror was designed to have a constant dispersion of -200 fs^2 over the highly reflective range as depicted in the figure. The maximum intensity enhancement calculated for a monochromatic input wave is shown for the two materials.

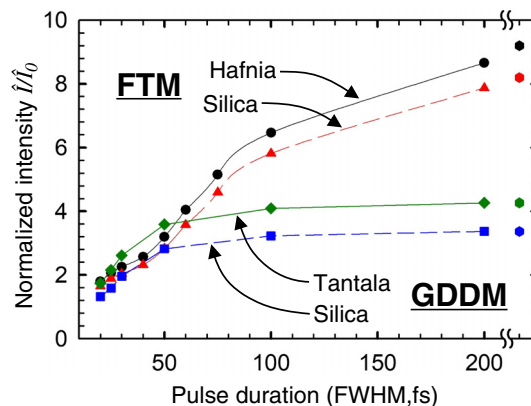


Fig. 2 Maximum intensity enhancement in the high-index and low-index layers for the FTM and GDDM as a function of the duration of the incident pulse. The data points on the far right show the enhancement values for monochromatic input.

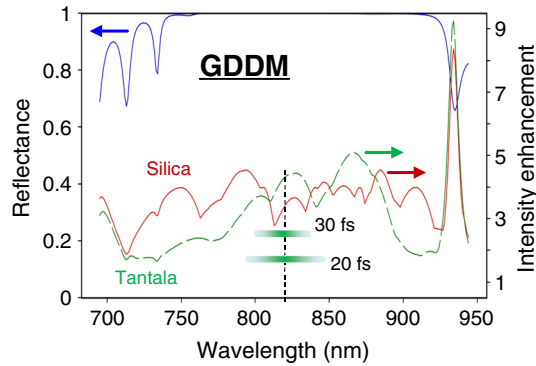


Fig. 3 Reflectance (blue, left axis) and monochromatic intensity enhancement (red for L-material and green for H-material, right axis) as a function of wavelength for the dispersive mirror (GDDM). The intensity enhancement values for a 20- and a 30-fs pulse are also shown (green horizontal bars). The horizontal extension of the bars represents the pulse spectrum. Their vertical position corresponds to the maximum intensity enhancement in the high-index material produced by these pulses.

At the points where the two curves intersect, the maximum intensity enhancement occurs at an interface between the two materials. At the center wavelength (820 nm), a maximum intensity enhancement of 4.2 occurs in the H-layer. For comparison, we show the values for a 20-fs (1.8) and a 30-fs (2.6) pulse calculated from the full spatiotemporal field evolution. Both intensity enhancements are significantly smaller than that obtained from the monochromatic approach. The histograms represent the bandwidth of the pulses.

Figures 2 and 3 show the change in maximum intensity enhancement, when considering the complete spectrum of the incident pulse. To also include the effect of the two different materials on the LIDT, we evaluated the figure of merit $M(z_m)$ according to Eq. (7) for mirrors (a) to (d), using the parameters from Ref. 5: $\kappa = 0.3$, $a = -0.16 \text{ J cm}^{-2} \text{ fs}^{-\kappa}$, $b = 0.074 \text{ J cm}^{-2} \text{ fs}^{-\kappa} \text{ eV}^{-1}$, and $E_g = (3.8, 5.1, 8.3) \text{ eV}$ for tantalum, hafnia, and silica, respectively. The results are shown in Fig. 4. The corresponding trend lines if \hat{Q}_{mon} (monochromatic limit) is used for the intensity enhancement are shown for comparison. The latter were obtained from Eq. (6) using $\tau_p(z) = \tau_p(0)$ and $\hat{I}(z) = \hat{I}_0 \hat{Q}_{\text{mon}}$.

As expected both approaches give very similar results for the QWM and the FEM as long as the pulse bandwidth does not exceed the mirror bandwidth. The situation is different for the GDDM and FTM. For shorter pulses, the simplified model can significantly overestimate the figure of merit because the intensity enhancement is larger and the pulse duration shorter than the actual values in the stack. This can lead to suboptimal performance of the mirror if the wrong merit function is used in the design.

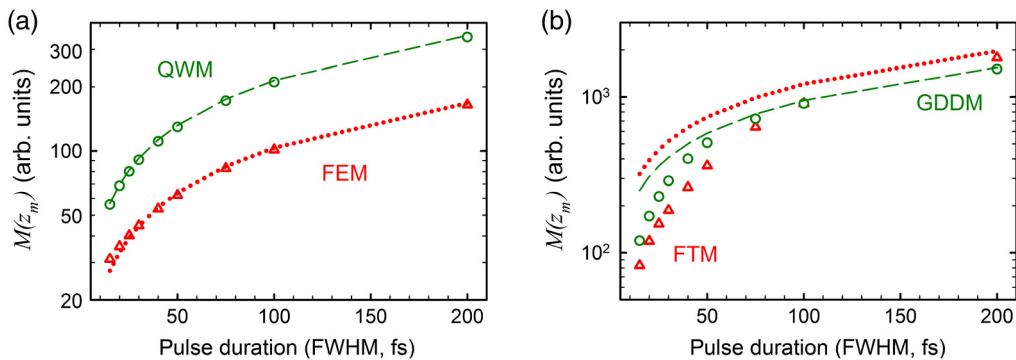


Fig. 4 Figure of merit $M(z_m)$ from Eq. (7) characterizing LIDT as a function of pulse duration. The dashed and dotted lines represent the predictions when the monochromatic intensity enhancement \hat{Q}_{mon} and $\tau_p(z) = \tau_p(0)$ are used. (a) QWM and FEM, (b) GDDM and FTM.

While a detailed test of our predictions is subject of future work, there are some observations that support the results discussed above. We measured the 1-on-1 and S-on-1 LIDT for the QWM and the FEM with 40-fs pulses at 815 nm, and a repetition rate of 1 kHz, and $S = 1000$. For both of these thresholds, we observed an increase in the fluence by a factor of about 2.2 (FEM versus QWM). This agrees well with the predicted factor of 2.05 from Fig. 4(a), where the figures of merits are 111 and 54 for QWM and FEM, respectively. For the FEM, the 1-on-1, S-on-1 LIDT fluence was $\sim 1.2 \text{ J/cm}^2$ and 1 J/cm^2 , respectively.

LID of the FTM is expected to occur at input fluences of about 70 mJ/cm^2 if we use $\hat{Q}_{\text{mon}} = 9.6$, the previously measured $F_c = 660 \text{ mJ/cm}^2$ for single hafnia films,⁵ and 40-fs pulses. Our actual measurements yielded an LIDT of $F_c = 290 \text{ mJ/cm}^2$, which is close to the prediction if we use the correct intensity enhancement for 40-fs input pulses of about 2.5, cf. Fig. 3. It should also be mentioned that an FTM designed with the correct intensity enhancement to predict LIDT produced a two times larger maximum conversion efficiency. Note, the latter is reached at input fluences just below LIDT.

4 Discussion and Summary

For high-reflectors and field-engineered variants that are based on quarterwave stacks, the pulse duration does not change in regions of large intensity enhancement as long as the mirror bandwidth is adequate. The maximum intensity enhancement is described well using monochromatic input.

In more complex structures, such as GDDMs and FTMs, the maximum intensity enhancement for pulses is smaller than its monochromatic counterpart. In addition, the pulse duration varies within the film sequence. In these mirrors, the pulse undergoes deformations (broadening), which are particularly pronounced near the field nodes where the intensity is low. As a general rule, the shorter the incident pulse, the larger the change of Q compared with monochromatic input.

We proposed a general approach to include LIDT information in the design of coating sequences for femtosecond mirrors using a figure of merit M . Necessary inputs are the spatio-temporal evolution of the laser pulse field inside the stack of coatings and the physical law governing damage of single layers. The widely used field-engineering based on the intensity enhancement calculated for monochromatic input is only valid for certain structures, such as HR quarterwave stacks and similar broad-bandwidth mirrors.

Our results suggest that LIDT optimization of mirrors with dispersive behavior such as GDDMs and FTMs require a figure of merit based on the actual pulse parameters inside the stack. A known phenomenological damage model for dielectric coatings for $\tau_p \geq 25 \text{ fs}$ was used to construct a figure of merit.⁵ While this LID model is likely valid also for shorter pulses, it becomes questionable for few-cycle pulses (sub-10-fs in the near IR). To first order, for such short pulses, peak intensity $I(z, t_m)$ and fluence $F(z)$ in the film stack are still meaningful quantities that will ultimately determine LID. It should be noted that even for sub-10 fs pulses, our approach accurately determines these two quantities for arbitrary film sequences.

Acknowledgments

We acknowledge support from the U.S. Department of Energy (DOE) under SBIR contract DE-SC0019788 and from Deutsche Forschungsgemeinschaft (DFG) within the Cluster of Excellence PhoenixD (390833453, EXC 2122). The authors declare no conflict of interest.

References

1. M. Jupé et al., "Mixed oxide coatings for advanced fs-laser applications," *Proc. SPIE* **6720**, 67200U (2008).
2. T. Willemsen et al., "Tunable optical properties of amorphous Tantalum layers in a quantizing structure," *Opt. Lett.* **42**(21), 4502–4504 (2017).

3. H. Xing et al., "Improving laser damage resistance of 355 nm high-reflective coatings by co-evaporated interfaces," *Opt. Lett.* **41**, 1253–1256 (2016).
4. L. A. Emmert and W. Rudolph, "Femtosecond laser-induced damage in dielectric materials," in *Laser-Induced Damage in Optical Materials*, D. Ristau, Ed., 1st ed., CRC Press (2014).
5. M. Mero et al., "Scaling laws of femtosecond laser pulse induced breakdown in oxide films," *Phys. Rev. B* **71**(11), 115109 (2005).
6. J. Jasapara et al., "Femtosecond laser pulse induced breakdown in dielectric thin films," *Phys. Rev. B* **63**(4), 45117–45117 (2001).
7. M. Grehn et al., "Enhancement of the damage resistance of ultra-fast optics by novel design approaches," *Opt. Express* **25**, 31948–31959 (2017).
8. J. H. Apfel, "Optical coating design with reduced electric field intensity," *Appl. Opt.* **16**(7), 1880–1885 (1977).
9. D. Schiltz et al., "Strategies to increase laser damage performance of Ta₂O₅/SiO₂ mirrors by modifications of the top layer design," *Appl. Opt.* **56**(4), C136–C139 (2017).
10. A. Hervy et al., "Femtosecond laser-induced damage threshold of electron beam deposited dielectrics for 1-m class optics," *Opt. Eng.* **56**(1), 011001 (2017).
11. M. Chorel et al., "Robust optimization of the laser induced damage threshold of dielectric mirrors for high power lasers," *Opt. Express* **26**(9), 11764 (2018).
12. S. Melnikas et al., "Enhancement of laser-induced damage threshold in chirped mirrors by electric field reallocation," *Opt. Express* **25**, 26537–26545 (2017).
13. M. T. O. Razskazovkaya et al., "Nonlinear absorbance in dielectric multilayers," *Optica* **2**, 803–811 (2015).
14. C. Rodríguez et al., "Frequency tripling mirror," *Opt. Express* **23**(24), 31594 (2015).
15. H. A. Macleod, *Thin-Film Optical Filters*, CRC Press (2017).
16. D. N. Nguyen et al., "Ti_xSi_{1-x}O₂ optical coatings with tunable index and their response to intense subpicosecond laser pulse irradiation," *Appl. Phys. Lett.* **93**, 261903 (2008).
17. T. Willemsen et al., "Enhancement of the damage resistance of ultra-fast optics by novel design approaches," *Opt. Express* **25**, 31948–31959 (2017).
18. C. Rodriguez and W. Rudolph, "Modeling third-harmonic generation from layered materials using nonlinear optical matrices," *Opt. Express* **22**(21), 25984–25992 (2014).
19. M. Lenzner, "Reflection off multilayers," January 2021, <http://www.lenzner.us/damage/> (accessed 8 February 2022).

Biographies of the authors are not available.